Chinese Chemical Letters 31 (2020) 2985–2987

Contents lists available at ScienceDirect

Chinese Chemical Letters

journal homepage: www.elsevier.com/locate/cclet

Communication

Direct observation of intramolecular coplanarity regulated polymorph emission of a tetraphenylethene derivative

Qingkai Qi[a,b,c,**], Shan Jiang[a], Qinglong Qiao[b], Jinbei Wei[a], Bin Xu[a], Xiaocun Lu[c,*], Zhaochao Xu[b,*], Wenjing Tian[a,*]

[a] State Key Laboratory of Supramolecular Structure and Materials, Jilin University, Changchun 130012, China
[b] CAS Key Laboratory of Separation Science for Analytical Chemistry, Dalian Institute of Chemical Physics, Chinese Academy of Sciences, Dalian 116023, China
[c] Department of Chemistry & Biomolecular Science, Clarkson University, Potsdam, NY 13699, United States

ARTICLE INFO

Article history:
Received 6 May 2020
Received in revised form 26 May 2020
Accepted 30 May 2020
Available online 1 June 2020

Keywords:
Tetraphenylethene
Polymorphism
Intramolecular coplanarity
Intermolecular stacking
Photophysical property

ABSTRACT

Polymorphism makes it possible to clarify the relationship between emission property and crystal structure. However, based on the exact molecular conformation in tetraphenylethene polymorphisms, it is still challenging to evaluate the difference of intramolecular coplanarity without the support of calculation because of the complex combination of four different torsion angles between four peripheral benzenes and the central ethylene plane. Here, by using a di-formyl-functionalized tetraphenylethene derivative, two ideal polymorphisms with a consistent trend of the corresponding torsion angles have been obtained. For the first time, we explicitly demonstrated that intramolecular coplanarity is the underlying cause of the polymorphism-dependent emission of tetraphenylethene derivatives.

Natural propeller-shaped tetraphenylethene (TPE), as one of the most well-known molecules with aggregation-induced emission (AIE) character, has received extensive attention during the past two decades [1–7]. The excellent AIE properties and high solid-state emission efficiency of TPE derivatives have enabled their wide usage in multiple fields, such as chemical sensors [8–14], organic light-emitting devices [15–18], biological labels [19–24], *etc*. For a long time, the structure-emission relationship of TPE has received broad research interests [25,26]. Synergetic effect of both the flexible molecular skeleton and hindered molecular rotation of the TPE unit makes it possible to exhibit multicolor emissions in solid state.

Recently, both our group and some other research groups have reported polymorphism-dependent emission of some TPE derivatives [27–32]. The structural analysis of polymorphisms provides an accessible way to reveal the relationship between photophysical property and crystal structure [33–37]. In general, the three-dimensional propeller-shaped TPE moiety can effectively avoid intermolecular π-π stacking and largely reduce its impact on the different polymorphic emission. Thus the intramolecular coplanarity becomes the main factor of different emission of TPE polymorphisms.

However, based on the precise molecular conformation of TPE polymorphisms, it is still challenging to evaluate the difference of molecular coplanarity without the support of calculation because of the complex combination of four different torsion angles between four peripheral benzenes and and the central ethylene plane (Fig. 1). We conducted data-mining in the Cambridge Crystallographic Data Center (CCDC) to measure all the four torsion angles in the reported polymorphisms of TPE derivatives with comprehensive statistical analysis (Table S1 in Supporting information). However, it was difficult to identify an ideal example in which all the torsion angles measured in polymorphic A are smaller (or larger) than polymorph B as shown in Fig. 1. In our previous works, we have to introduce bond length alternation (BLA), a key parameter determining the bandgap and degree of π-conjugation, to compare the coplanarity difference in both methoxy- and dimethylamino-substituted TPE polymorphisms [27,28]. So far there is no direct observation to confirm that the different intramolecular coplanarity is the profound reason for the polymorphism-dependent emission of TPE derivates.

In this work, by using a di-formyl-functionalized TPE derivative, (*E*)-TPE-2CHO, two ideal polymorphisms with a consistent trend of the corresponding torsion angles have been obtained. For the first time, we explicitly demonstrated that intramolecular coplanarity is responsible for their different emissions of polymorphisms.

* Corresponding authors.
** Corresponding author at: State Key Laboratory of Supramolecular Structure and Materials, Jilin University, Changchun 130012, China.
E-mail addresses: qqi@clarkson.edu (Q. Qi), xlu@clarkson.edu (X. Lu), zcxu@dicp.ac.cn (Z. Xu), wjtian@jlu.edu.cn (W. Tian).

https://doi.org/10.1016/j.cclet.2020.05.044

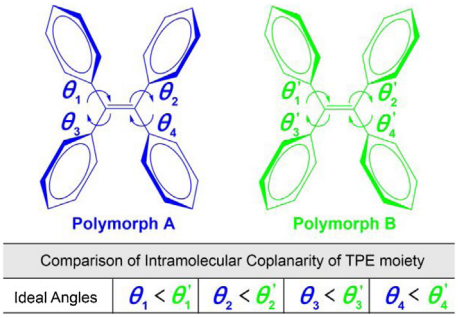

Fig. 1. Schematic diagram of the comparison of intramolecular coplanarity of the TPE moiety in polymorphisms.

Detailed synthesis and characterization of (*E*)-TPE-2CHO have been included in Supporting information. Two different polymorphs of (*E*)-TPE-2CHO were obtained at the same time by slow evaporation of their ethyl acetate/*n*-hexane solutions at room temperature, which enables further confirmation of the molecular structure by the crystallographic analysis (Table S2 in Supporting information). Their ORTEP drawings are shown in Figs. 2a and b. As shown in Figs. 2c and d, the two polymorphs showed totally different emission colors under a 365 nm UV light. Photoluminescence spectra of the two polymorphs revealed that one crystal emitted a cyan emission peaked at 478 nm and another emitted a green emission peaked at 503 nm (Fig. 2e); the emission peak difference between the two polymorphs was about 25 nm. The two polymorphic crystals were named as (*E*)-TPE-2CHO-Cyan and (*E*)-TPE-2CHO-Green according to their molecular structure and emission colors respectively. Then, the UV–vis reflection spectra of the two polymorphs were used to explore their emission difference (Fig. 2f). Comparing with the absorption of (*E*)-TPE-2CHO-Cyan, (*E*)-TPE-2CHO-Green showed an emerging red-shifted absorption band centered at about 406 nm, which indicated that (*E*)-TPE-2CHO-Green may have a more extended π-conjugation. Additionally, the other photophysical parameters of two polymorphs including the fluorescence quantum yield (Φ_F) and average lifetime ($<\tau>$, Fig. S1 in Supporting information) were measured, from which the radiative transition rate and non-radiative transition rate constant can be easily calculated (Table 1). Unlike their quite different emission and UV–vis reflection spectra, all these parameters of the two polymorphs make little difference.

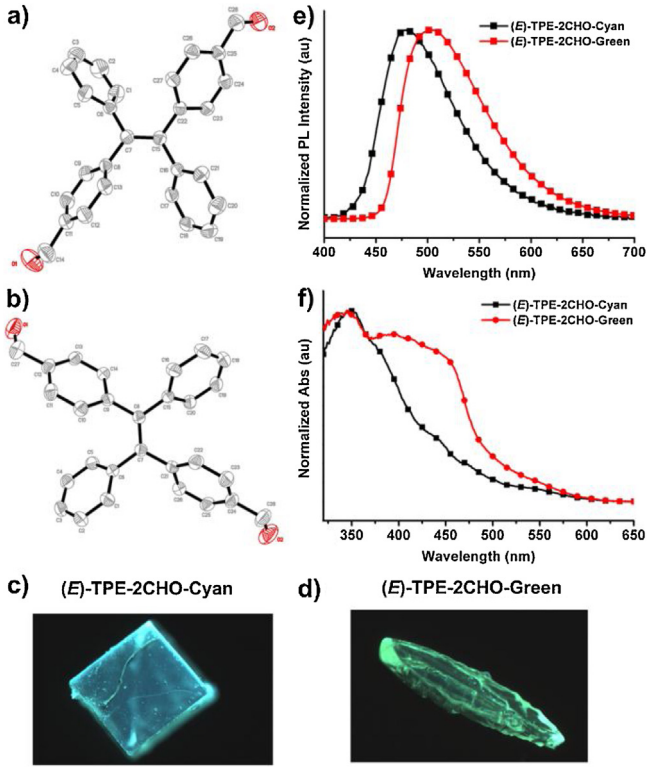

Fig. 2. (a, b) ORTEP drawings (50 % probability ellipsoids) and the numbering schemes for the two polymorphs. (c, d) PL images of the two crystals taken under a 365 nm UV light. (e, f) PL spectra and UV–vis reflection spectra of the two polymorphs.

We further did a structural analysis of the two polymorphs to establish the relationship between crystal structures and optical spectra. Each unit cell consisted of four and two independent molecules for (*E*)-TPE-2CHO-cyan and (*E*)-TPE-2CHO-green respectively (Figs. 3a and b). No intermolecular π-π interaction between the adjacent molecules was found in the two polymorphs, which was due in part to the steric hindrance resulted from the highly twisted TPE configuration. Indeed, there were many weak supramolecular interactions such as C–H···O and C–H···π in the two crystals, and their detailed distances and angles are summarized in Figs. 3c and d. The network of weak supramolecular interactions together contributed to the formation of two single crystals. Besides, we further measured the corresponding dihedral angles between the four peripheral benzenes and ethylene planes, as well as benzenes and the aldehyde groups. As shown in Figs. 3e and f, all the measured dihedral angles between the four benzene rings and central ethylene plane in (*E*)-TPE-2CHO-Cyan (48.39°, 49.95°, 63.26°, 54.44°) are larger than the corresponding dihedral angles of (*E*)-TPE-2CHO-Green (44.53°, 49.29°, 47.66°, 50.71°). It is worth mentioning that this is the first experimental proof to illustrate intramolecular coplanarity-directed bathochromic shift in TPE polymorphisms.

Furthermore, the DSC curves of the two polymorphisms were measured (Fig. S2 in Supporting information), and the melting point of (*E*)-TPE-2CHO-Green (174.7 °C) was slightly lower than that of (*E*)-TPE-2CHO-Cyan (178.0 °C), indicating that the green crystal has less crystal lattice energy. The bandgaps of the single (*E*)-TPE-2CHO molecule were calculated based on the exact molecular configurations in the two polymorphisms without geometry optimizations using B3LYP/6-31 G(d,p) by Gaussian 09 [38], and the results are given in Fig. 4. The calculated bandgap of the single molecule in the cyan crystal (3.97 eV) is larger than the green crystal (3.68 eV), which is consistent with the bathochromic shift of the UV–vis reflection and emission spectra of the two polymorphisms (Figs. 2e and f).

In summary, we obtained two polymorphic crystals of a diformyl-functionalized TPE derivative ((*E*)-TPE-2CHO) with a feature of intramolecular coplanarity-directed emission colors. All the photophysical parameters of the two polymorphic crystals were measured and comparatively studied. After comprehensive analysis of the intermolecular stacking and intramolecular conformation of the two crystals, we clearly illustrated that the polymorph-dependent emission difference of (*E*)-TPE-2CHO is merely due to the twisted degree difference of the central TPE core. Herein, we obtained direct observation that the intramolecular coplanarity difference of the central TPE unit results in the

Table 1
Summary of photophysical parameters of two polymorphs.

Crystal	λ_{abs} (nm)	λ_{em} (nm)	Φ_F (%)	$<\tau>$ (ns)	K_r (s^{-1})	K_{nr} (s^{-1})
Cyan	347	478	65.4	3.06	2.137×10^8	1.131×10^8
Green	347/406	503	65.2	2.91	2.241×10^8	1.196×10^8

Abbreviations: Φ_F: fluorescence quantum yield determined using a calibrated integrating sphere; average lifetime: $<\tau>$; radiative transition rate constant: $K_r = \Phi_F / <\tau>$; non-radiative transition rate constant: $K_{nr} = (1-\Phi_F)/<\tau>$.

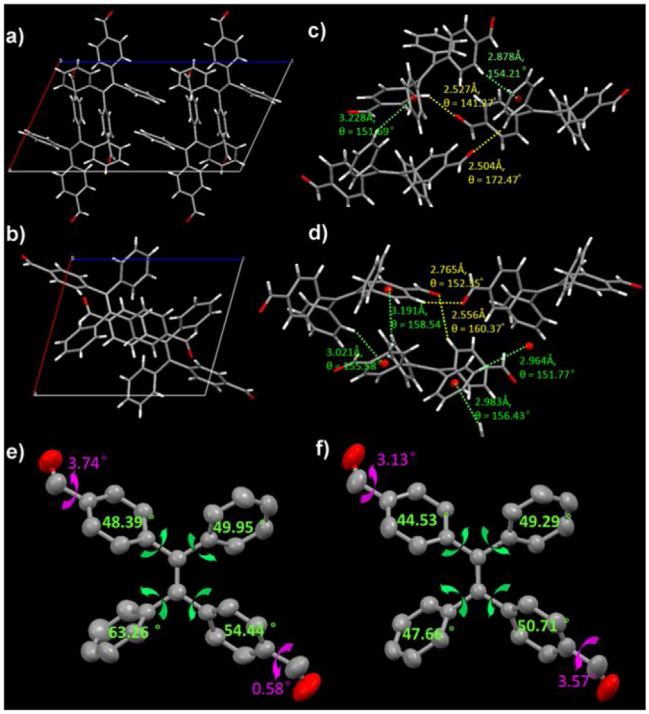

Fig. 3. Polymorph structural analysis of (*E*)-TPE-2CHO-cyan (a, c, e) and (*E*)-TPE-2CHO-green (b, d, f): (a, b) Unit cell structures viewed along b-axis; (c, d) the existed weak interactions and corresponding angles: C–H···π (green line) and C-H···O (yellow line); (e, f) selected torsion angles (degree).

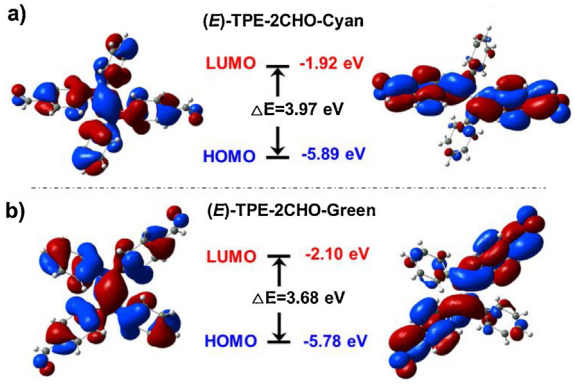

Fig. 4. Molecular orbital amplitude plots of HOMO and LUMO energy levels of crystals (*E*)-TPE-2CHO-Cyan (a) and (*E*)-TPE-2CHO-Green (b) calculated using B3LYP/6-31 G(d,p) by Gaussian 09.

different emission of polymorphisms. This work will enhance the fundamental understanding of the relationship between crystal structures and photophysical properties for various AIE luminogens.

Declaration of competing interest

The authors declare that they have no known competing financial interests or personal relationships that could have appeared to influence the work reported in this paper.

Acknowledgments

This work was supported by the National Natural Science Foundation of China (Nos. 21708039, 21878286, 21908216, 21835001, 21875085, 51773080, 21674041), and the Program for Changbaishan Scholars of Jilin Province.

Appendix A. Supplementary data

Supplementary material related to this article can be found, in the online version, at doi:https://doi.org/10.1016/j.cclet.2020.05.044.

References

[1] Z. Li, Y. Huo, X. Yang, et al., Chin. J. Org. Chem. 36 (2016) 2317–2332.
[2] M. Wang, G. Zhang, D. Zhang, et al., J. Mater. Chem. 20 (2010) 1858–1867.
[3] Y.G. He, S.Y. Shi, N. Liu, et al., Macromolecules 49 (2016) 48–58.
[4] X. Zhang, K. Wang, M. Liu, et al., Nanoscale 7 (2015) 11486–11508.
[5] J. Yu, C. Tang, X. Gu, et al., Chem. Commun. 56 (2020) 3911–3914.
[6] X. Han, B. Zhang, J. Chen, et al., J. Mater. Chem. B 5 (2017) 5096–5100.
[7] X. Han, D. Li, X. Ma, et al., New J. Chem. 42 (2018) 6609–6612.
[8] C. Zhang, Y. Li, X. Xue, et al., Chem. Commun. 51 (2015) 4168–4171.
[9] X.G. Liu, H. Wang, B. Chen, et al., Chem. Commun. 51 (2015) 1677–1680.
[10] H. Zhou, F. Liu, X. Wang, et al., J. Mater. Chem. C 3 (2015) 5490–5498.
[11] Y. Xie, Z. Li, Chem. Asian J. 14 (2019) 2524–2541.
[12] N. Jiang, Y. Wang, A. Qin, et al., Chin. Chem. Lett. 30 (2019) 143–148.
[13] L. Ma, C. Li, Q. Yan, et al., Chin. Chem. Lett. 31 (2020) 361–364.
[14] N. Liu, L. Shi, X. Han, et al., Chin. Chem. Lett. 31 (2020) 386–390.
[15] L. Chen, Y. Jiang, H. Nie, et al., ACS Appl. Mater. Interface 6 (2014) 17215–17225.
[16] Z. Zhao, J.W.Y. Lam, B.Z. Tang, J. Mater. Chem. 22 (2012) 23726–23740.
[17] H. Zhang, J. Zhou, G.G. Shan, et al., Chem. Commun. 55 (2019) 12328–12331.
[18] Z. Lu, Y. Cheng, W. Fan, et al., Chem. Commun. 55 (2019) 8474–8477.
[19] Z. Wang, T.Y. Yong, J. Wan, et al., ACS Appl. Mater. Interface 7 (2015) 3420–3425.
[20] W. Zhang, R.T.K. Kwok, Y. Chen, et al., Chem. Commun. 51 (2015) 9022–9025.
[21] H. Wang, G. Liu, H. Gao, et al., Polym. Chem. 6 (2015) 4715–4718.
[22] W. Shen, J. Yu, J. Ge, et al., ACS Appl. Mater. Interface 8 (2016) 927–935.
[23] S. Li, Y. Shang, E. Zhao, et al., J. Mater. Chem. C 3 (2015) 3445–3451.
[24] Z. Zhao, B. Chen, J. Geng, et al., Part. Part. Syst. Charact. 31 (2014) 481–491.
[25] J. Shi, N. Chang, C. Li, et al., Chem. Commun. 48 (2012) 10675–10677.
[26] J. Mei, Y. Hong, J.W.Y. Lam, et al., Adv. Mater. 26 (2014) 5429–5479.
[27] Q. Qi, Y. Liu, X. Fang, et al., RSC Adv. 3 (2013) 7996–8002.
[28] Q. Qi, J. Zhang, B. Xu, et al., J. Phys. Chem. C 117 (2013) 24997–25003.
[29] S. Jiang, J. Wang, Q. Qi, et al., Chem. Commun. 55 (2019) 3749–3752.
[30] N. Zhao, Z. Yang, J.W.Y. Lam, et al., Chem. Commun. 48 (2012) 8637–8639.
[31] M. Khorloo, Y. Cheng, H. Zhang, et al., Chem. Sci. 11 (2020) 997–1005.
[32] Q. Yang, D. Li, W. Chi, et al., J. Mater. Chem. C 7 (2019) 8244–8249.
[33] H.Y. Zhang, Z.L. Zhang, K.Q. Ye, et al., Adv. Mater. 18 (2006) 2369–2372.
[34] T. Mutai, H. Tomoda, T. Ohkawa, et al., Angew. Chem. Int. Ed. 47 (2008) 9522–9524.
[35] M. Brinkmann, G. Gadret, M. Muccini, et al., J. Am. Chem. Soc. 122 (2000) 5147–5157.
[36] K. Wang, H. Zhang, S. Chen, et al., Adv. Mater. 26 (2014) 6168–6173.
[37] Q. Zhu, Y. Zhang, H. Nie, et al., Chem. Sci. 6 (2015) 4690–4697.
[38] M.J. Frisch, G.W. Trucks, H.B. Schlegel, et al., Gaussian 09, Revision D.01, Gaussian, Inc., Wallingford, CT, 2013.